LASER SPECTROSCOPY

PACS numbers: 42.55.Rz; 42.62.Fi
DOI: 10.1070/QE2005v035n05ABEH006589

Spectral dynamics of intracavity absorption in a pulsed Cr^{2+} : ZnSe laser

V.A. Akimov, V.I. Kozlovskii, Yu.V. Korostelin, A.I. Landman, Yu.P. Podmar'kov, M.P. Frolov

***Abstract*. The growth dynamics of intracavity absorption is studied during recording line absorption spectra by the method of intracavity laser spectroscopy using a pulsed Cr^{2+} : ZnSe laser tunable between 2.1 and 3.1 μm. In the lasing duration range from 0 to 235 μs, an intracavity absorption signal increases linearly with time, providing the effective absorption length of 70 km.**

Keywords: *intracavity laser spectroscopy, solid-state lasers, Cr^{2+} : ZnSe laser.*

1. Introduction

Intracavity laser spectroscopy (ILS) [1] is one of the highly sensitive methods of absorption analysis along with acousto-optic spectroscopy, diode spectroscopy, and intracavity radiation decay spectroscopy [2–4]. A further development of these promising methods for a rapid control of gaseous media depends to a great extent on the elaboration of new IR lasers emitting in the spectral region where vibrational absorption transitions of many molecules lie. In this connection solid-state lasers based on chalcogenide single crystals (ZnS, ZnSe, CdSe, etc.) doped with transition-metal ions [5], in particular, Cr^{2+} attract great interest.

We have shown in our previous paper [6] that a Cr^{2+} : ZnSe laser allows the extension of ILS to the spectral range from 2.1 to 3.1 μm. We have recorded the intracavity absorption spectra of atmospheric water vapour for the duration of emission from a Cr^{2+} : ZnSe laser not exceeding 100 μs [6]. We obtained only qualitative results because the recorded absorption lines were strongly saturated and the laser emission spectrum contained strong parasitic modulation caused by the interference of laser emission from cavity elements, in particular, from a Cr^{2+} : ZnSe crystal, whose faces formed a Fabry–Perot etalon of thickness 3 mm.

V.I. Kozlovskii, Yu.V. Korostelin, A.I. Landman, Yu.P. Podmar'kov, M.P. Frolov P.N. Lebedev Physics Institute, Russian Academy of Sciences, Leninskii prosp. 53, 119991 Moscow, Russia;
e-mail: frolovmp@x4u.lebedev.ru;
V.A. Akimov Moscow Institute of Physics and Technology (State University), Institutskii per. 9, 141700 Dolgoprudnyi, Moscow region, Russia

Received 23 March 2005
Kvantovaya Elektronika **35** (5) 425–428 (2005)
Translated by M.N. Sapozhnikov

Hole burning in the emission band of a broadband laser in the ILS method is described by the modified Bouguer–Lambert–Beer law [7]

$$\frac{I(\omega)}{I_0(\omega)} = \exp\left[-\frac{k(\omega)ctL_a}{L_c}\right], \quad (1)$$

where $I(\omega)$ is the lasing intensity at the frequency ω at the instant t; $I_0(\omega)$ is the spectral distribution envelope of emission at the frequency ω; $k(\omega)$ is the absorption coefficient; c is the velocity of light; L_a is the physical length of an intracavity absorbing layer (for example, the length of an intracavity cell with an absorbing material); and L_c is the total cavity length. The time dependence of $\ln[I_0(\omega)/I(\omega)]$ is linear, the intracavity absorption signal increases linearly with the lasing duration, and expression (1) can be used for quantitative ILS measurements. However, this is valid only for a certain duration of lasing, which depends on the properties of a particular active medium. For example, when solid-state lasers were used in the ICL method, a linear increase of the absorption signal for a neodymium glass laser was experimentally observed during 12 ms [8], for $Ti^{3+}:Al_2O_3$ during 4.5 ms [7], and for $Co^{2+}:MgF_2$ laser during 4 ms [9]. For each new broadband laser used in ILS measurements, the validity of expression (1) should be verified experimentally.

In this paper, the Cr^{2+} : ZnSe laser pulse duration was increased compared to that used in [6] and interference effects were considerably reduced, which allowed us to measure quantitatively the dynamics of intracavity absorption in the emission spectrum of the Cr^{2+} : ZnSe laser in the 0–235-μs range.

2. Experimental setup

The scheme of the experimental setup is presented in Fig. 1. Unlike [6], the Cr^{2+} : ZnSe laser was placed inside a hermetic chamber whose windows were used as cavity mirrors. The chamber was connected to a vacuum system and could be pumped and filled with a mixture of the required composition. The laser cavity of length 365 mm was formed by spherical mirrors M1 and M2 with the radius of curvature 200 mm.

The active element of the laser of thickness 8.7 mm was made of a Cr^{2+} : ZnSe single crystal grown by the seeded physical vapour transport method in helium and doped directly during the growth [10, 11]. It was placed in the middle of the cavity at the Brewster angle. The use of a thicker crystal than in [6] considerably reduced the mod-

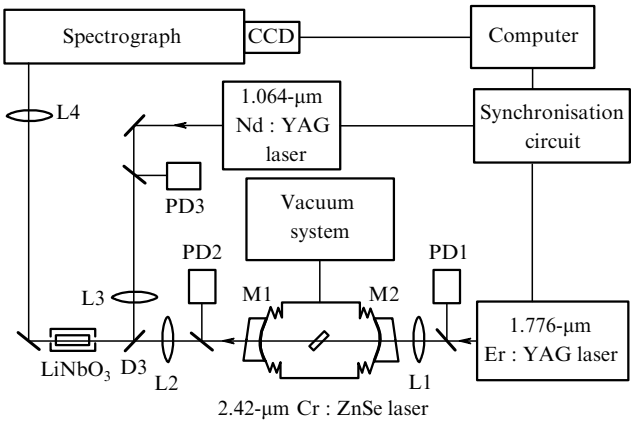

Figure 1. Scheme of the experimental setup.

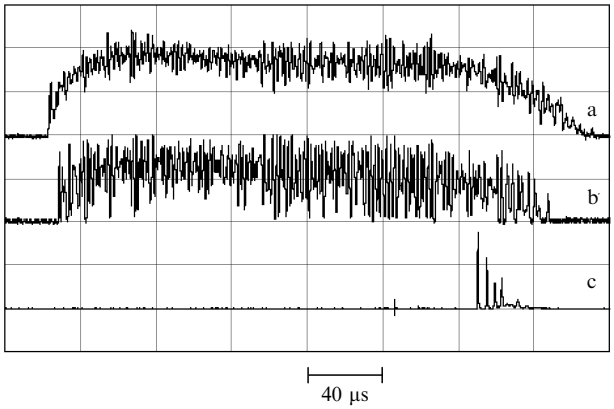

Figure 2. Time scans of the pump (a), Cr^{2+} : ZnSe (b) and Nd:YAG (c) laser pulses. The sweep speed is 40 μs div^{-1}.

ulation of the emission spectrum of the laser caused by interference effects. As the crystal thickness is increased, the distance between the main laser beam and secondary beams reflected from crystal faces increases. As a result, the overlap of interfering beams decreases and the modulation amplitude of the spectrum becomes lower.

The Cr^{2+} : ZnSe laser was longitudinally pumped at 1.776 μm by an Er : YAG laser, whose radiation was focused by lens L1. Because the maximum of the absorption band of the Cr^{2+} : ZnSe crystal lies near 1.8 μm [5], the Er : YAG laser provided more efficient pumping than a 1.95-μm Co : MgF_2 laser used in [6]. The spectral dynamics of the Cr^{2+} : ZnSe laser was studied upon pumping approximately twice as large as the lasing threshold.

The IR emission spectrum of the Cr^{2+} : ZnSe laser was recorded by converting the laser radiation to a shorter-wavelength region (739 nm) by the nonlinear-optical method (up-conversion) in a $LiNbO_3$ crystal (temperature-controlled 90° phase matching), which allowed the use of a grating spectrograph equipped with a CCD linear array. The nonlinear-optical conversion of broadband IR radiation was performed by mixing it with monochromatic radiation from a 1.064-μm Nd : YAG laser with the linewidth no more than 0.02 cm^{-1}. The beams from the Cr^{2+} : ZnSe and Nd:YAG lasers were focused and made coincident inside the $LiNbO_3$ crystal with the help of lenses L2 and L3 and dichroic mirror D3. The converted radiation was separated with a glass optical filter and focused by lens L4 on the entrance slit of the grating spectrograph with a theoretical resolution of 0.035 cm^{-1}. The centre of the emission spectrum of the Cr^{2+} : ZnSe laser determined by the spectral properties of cavity mirrors and the gain spectrum was located at 2.42 μm.

Photodiodes PD1, PD2, and PD3 were used to record the shapes of pulses emitted by the Er : YAG, Cr^{2+} : ZnSe, and Nd : YAG lasers, respectively, and for measuring the relative delay of pulses from the Cr^{2+} : ZnSe and Nd : YAG lasers. Typical oscillograms are presented in Fig. 2. A short duration of the Nd : YAG laser pulse (~ 15 μs) compared to that of the Cr^{2+} : ZnSe laser (~ 250 μs) allowed the time-resolved recording of the spectra by delaying with the help of the synchronisation circuit a pulse from the Nd : YAG laser by the time t with respect to the leading edge of a pulse from the Cr^{2+} : ZnSe laser. In this way, we observed the development of intracavity absorption in time. The delay instability did not exceed ±3 μs.

3. Experimental results and discussion

Figure 3 shows the emission spectra of the Cr^{2+} : ZnSe laser, whose cavity was filled with atmospheric air at a pressure of 1 atm, recorded at different instants. Each spectrum was obtained by summation over 100 laser pulses. A comparison of these spectra with similar spectra obtained earlier [6] shows that the use of a thicker active crystal considerably reduces the modulation of the spectrum caused by interference effects. Holes in the spectra correspond to the absorption lines of atmospheric water vapour. One can see from Fig. 3 that the emission spectrum narrows down with time, while the spectral holes increase, which is typical of the ILS method. However, we failed to

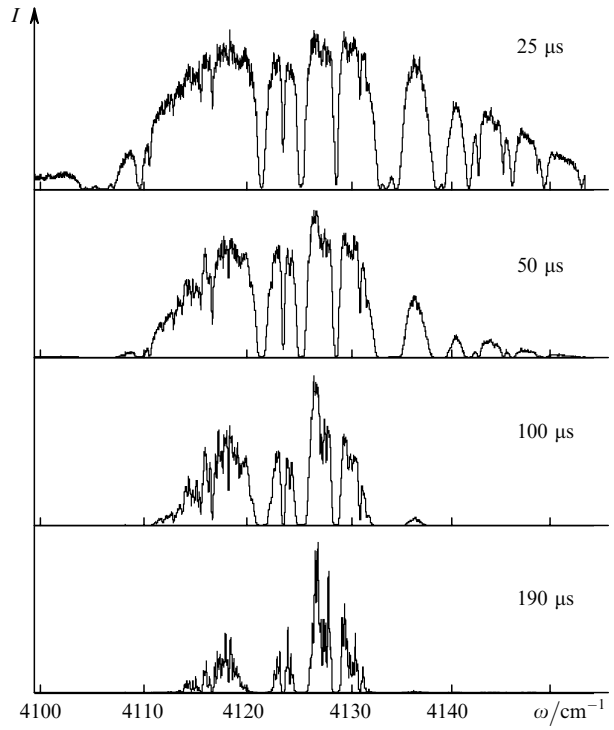

Figure 3. Emission spectra of the Cr^{2+} : ZnSe laser with the cavity filled with atmospheric air at a pressure of 1 atm, recorded at different lasing instants.

process the spectra quantitatively because of a very strong saturation of the absorption lines of atmospheric water vapour.

We attempted to work at reduced pressures of air in the cavity, which in principle allowed the lowering of the partial pressure of water vapour, thereby eliminating the saturation of absorption spectra. However, the width of absorption lines at low air pressures became smaller than the instrumental function width of our spectrograph, which severely complicated the data processing. In addition, the study of water vapour as an absorbing gas did not give reliable quantitative results on the dynamics of intracavity absorption because we have failed to provide a constant partial pressure of water vapour due to water deposition on the cavity chamber walls and evaporation.

CO, which has many absorption lines in the vicinity of 2.42 μm [12], proved to be more convenient as an absorbing gas. The Cr^{2+} : ZnSe laser cavity was filled with a preliminary prepared mixture of the $CO : N_2 = (1.00 \pm 0.05) : 10000$ composition. This allowed us to record the unsaturated intracavity absorption lines of CO of width exceeding the spectral resolution of our spectrograph by several times at the total pressure of the mixture 1–2 atm over the entire range of lasing duration.

We recorded the emission spectra of the Cr^{2+} : ZnSe laser with the cavity filled with this mixture in the range of lasing duration from 0 to 250 μs. Figure 4 shows some of these spectra obtained for the total pressure of the mixture equal to 1.5 atm at the lasing instants 60, 110, and 210 μs. Each spectrum was obtained by summation over 100 laser pulses. The holes observed in the spectra are caused by the CO absorption lines (also several H_2O absorption lines are present) [12]. Measurements were performed for the 4127.1376 cm^{-1} ($^{13}C\,^{16}O$), 4131.3964 cm^{-1} ($^{13}C\,^{16}O$), and 4132.1542 cm^{-1} ($^{12}C\,^{16}O$) absorption lines of CO [12] indicated by circles in Fig. 4. Note that the natural content of $^{13}C\,^{16}O$ in CO is 1.1%, i.e., the content of $^{13}C\,^{16}O$ molecules in the mixture under study is 1.1×10^{-4} %.

Having processed the results obtained, we plotted the dependences of $\ln[I_0(\omega)/I(\omega)]$ on time for the centres of all the three lines of CO (Fig. 5), which are well approximated by straight lines over the entire range of lasing duration (0–235 μs). This means that the use of the Cr^{2+} : ZnSe laser for ICL measurements provides the effective absorption length no less than 70 km. Such an effective absorption length ensures the recording of weak absorption lines with the absorption coefficient of 10^{-8} cm^{-1}. This sensitivity allows one, for example, to detect impurity CO molecules at a level of 2×10^{-8} by using the most intense absorption lines lying within the emission spectrum of the Cr^{2+} : ZnSe laser.

By using the experimental data obtained and the values of the intensity and broadening coefficients of the lines from [12], we determined the concentrations of $^{12}C\,^{16}O$ and $^{13}C\,^{16}O$ in the cavity at the total mixture pressure of 1.5 atm. We assumed that the absorption line broadening by nitrogen weakly differs from that by air. The concentration of $^{12}C\,^{16}O$ measured in this way was $(3.85 \pm 0.38) \times 10^{15}$ cm^{-3}, in good agreement with the value $(3.7 \pm 0.19) \times 10^{15}$ cm^{-3} determined from the initial composition of the mixture. In this case, the content of $^{13}C\,^{16}O$ with respect to $^{12}C\,^{16}O$ was (1.20 ± 0.17) %, which is close to the natural content. The measurement error was mainly determined by the spectral noise of the Cr^{2+} : ZnSe laser and the

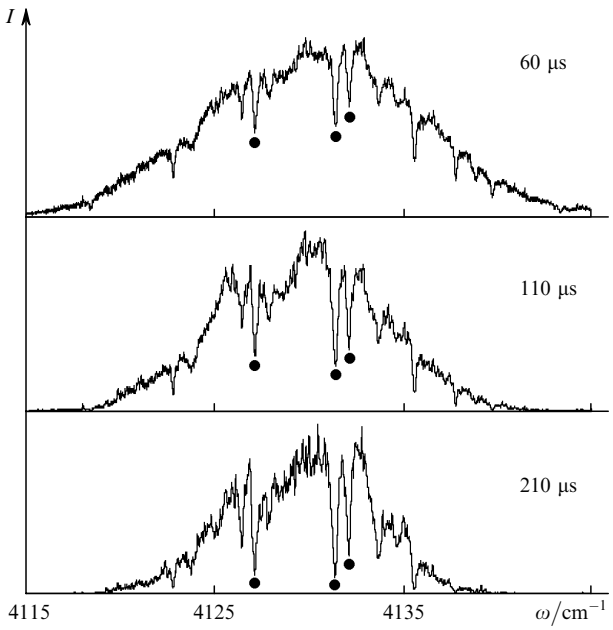

Figure 4. Emission spectra of the Cr^{2+} : ZnSe laser with the cavity filled with the $CO : N_2 = 1 : 10000$ mixture at a pressure of 1.5 atm, recorded at different lasing instants. The circles indicate the CO absorption lines.

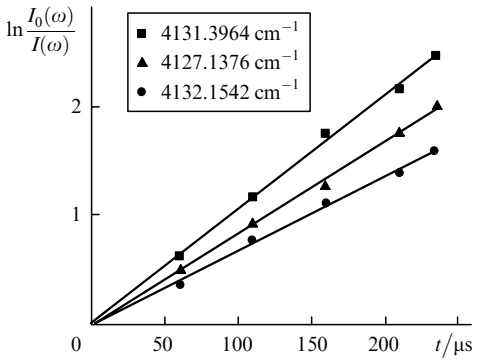

Figure 5. Dependences of the intracavity absorption signals on the generation time of the Cr^{2+} : ZnSe laser plotted for the three CO absorption lines.

instability of the Nd : YAG laser pulse delay with respect to the leading edge of the Cr^{2+} : ZnSe laser pulse. The latter factor is caused by the imperfection of our equipment and can be easily removed. As for the spectral noise, it can be substantially suppressed by increasing the number of summated pulses; however, this will require an increase in the averaging time or pulse repetition rate.

The Cr^{2+} : ZnSe laser pulse duration considered in this paper was limited by the pulse duration of our pump laser. However, it is known that a Cr^{2+} : ZnSe laser can operate in the cw regime as well [13]. This suggests that even higher sensitivity can be achieved in the future.

4. Conclusions

We have shown that intracavity absorption in the emission spectrum of a broadband Cr^{2+} : ZnSe laser develops linearly with time at least up to 235 μs. In this case, the equivalent length of an absorbing layer equal to 70 km is achieved. If the noise level in the emission spectrum does not exceed 10 % (which is provided by averaging over

~ 100 pulses), weak absorption lines with the absorption coefficient $\sim 10^{-8}$ cm^{-1} can be recorded within the emission spectrum of the Cr^{2+} : ZnSe laser (2.1 – 3.1 μm).

Acknowledgements. This work was partially supported by the American Civilian Research and Development Foundation (Grant CRDF BRHE REC-011), the New Materials and Structures Program, RAS, and the Development of the Scientific Potential of the Higher School Program, the Ministry of Education and Science of the Russian Federation (Project No. 37900).

References

1. Pakhomycheva L.A., Sviridenkov E.A., Suchkov A.F., Titova L.V., Churilov S.S. *Pis'ma Zh. Eksp. Teor. Fiz.*, **12**, 60 (1970).
2. Sigrist M.W., Bohren M.W., Calasso I.G., Nagele M., Romann M., Seiter M. *Proc. SPIE Int. Soc. Opt. Eng.*, **4063**, 17 (2000).
3. Werle P., Popov A. *Appl. Opt.*, **38**, 1494 (1999).
4. Berden G., Peeters R., Meijer G. *Int. Rev. Phys. Chem.*, **19**, 565 (2000).
5. DeLoach L.D., Page R.H., Wilke G.D., Payne S.A., Krupke W.F. *IEEE J.Quantum Electron.*, **32**, 885 (1996).
6. Akimov V.A., Kozlovskii V.I., Korostelin Yu.V., Landman A.I., Podmar'kov Yu.P., Frolov M.P. *Kvantovaya Elektron.*, **34**, 185 (2004) [*Quantum Electron.*, **34**, 185 (2004)].
7. Baev V.M., Latz T., Toschek P.E. *Appl. Phys. B*, **69**, 171 (1999).
8. Baev V.M., Dubov V.P., Sviridenkov E.A. *Kvantovaya Elektron.*, **12**, 2490 (1985) [*Sov. J. Quantum Electron.*, **15**, 1648 (1985)].
9. Frolov M.P., Podmar'kov Yu.P., Raspopov N.A. *Proc. SPIE Int. Soc. Opt. Eng.*, **4766**, 133 (2002).
10. Kozlovskii V.I., Korostelin Yu.V., Landman A.I., Podmar'kov Yu.P., Frolov M.P. *Kvantovaya Elektron.*, **33**, 408 (2003) [*Quantum Electron.*, **33**, 408 (2003)].
11. Kozlovskii V.I., Korostelin Yu.V., Landman A.I., Podmar'kov Yu.P., Frolov M.P. *Poverkhnost'*, (9), 26 (2004).
12. The HITRAN database, 2004 edition (www.hitran.com).
13. Wagner G.J., Carrig T.J., Page R.H., Schaffers K.I., Ndap J.-O., Ma X., Burger A. *Opt. Lett.*, **24**, 19 (1999).